

Classification of interfacial water governed by water-polymer interactions in hydrated polymers: A molecular dynamics simulation study of ethylene-based and acrylate polymers

Atsuki Hashimoto, Kokoro Shikata, Kang Kim,^{a)} and Nobuyuki Matubayasi^{b)}

Division of Chemical Engineering, Department of Materials Engineering Science, Graduate School of Engineering Science, The University of Osaka, Toyonaka, Osaka 560-8531, Japan

(Dated: 27 March 2026)

We perform molecular dynamics simulations to investigate hydration structures and dynamics in seven water-containing polymers: poly(vinyl alcohol) (PVA), poly(2-hydroxyethyl acrylate) (PHEA), poly(2-hydroxyethyl methacrylate) (PHEMA), poly(butyl acrylate) (PBA), poly(2-methoxyethyl methacrylate) (PMEMA), poly(ethylene glycol) (PEG), and poly(2-methoxyethyl acrylate) (PMEA). The analysis integrates four perspectives: the water-content dependence of the glass transition temperature T_g , polymer chain fluctuations characterized by dihedral angle distributions, hydrogen-bond lifetimes τ_{HB} between water and polymer functional groups, and the localization and exchange dynamics of confined water quantified by the distinct part of van Hove correlation function. Hydroxyl-containing polymers (PVA, PHEA, and PHEMA) exhibit relatively high dry-state T_g values and its pronounced depression upon hydration. Chain fluctuations are limited, and τ_{HB} follows Arrhenius behavior, forming localized hydration shells. In contrast, PMEMA and PBA show low equilibrium water contents and hydrophobic character; although their dry-state T_g values are moderately lower and less sensitive to water content, chain fluctuations remain small, and τ_{HB} also obeys Arrhenius behavior, with hydrophobic aggregation promoting water localization. PEG and PMEA display low dry-state T_g values and weak water-content dependence. Greater rotational freedom around ether or methoxy oxygen atoms leads to larger chain fluctuations and loosely bound water. Below T_g , τ_{HB} between water and ether or methoxy oxygen atoms exhibits super-Arrhenius behavior. These results clarify three hydration types: highly hydrated (PVA, PHEA, and PHEMA), hydrophobic (PMEMA and PBA), and flexibly hydrated (PEG and PMEA), and provide a molecular-level framework for interpreting interfacial water governed by water-polymer interactions.

I. INTRODUCTION

Water molecules at polymer interfaces in aqueous environments play a central role in determining polymer functionality. Under hydrated conditions, polymers exhibit behaviors such as swelling, which enables functional applications including hydrogels for drug delivery and contact lenses, temperature-responsive materials, and membranes for selective separation.¹ Interfacial water is located near polymer surfaces through intermolecular forces such as van der Waals interactions, electrostatic interactions, and hydrogen bond (H-bond) with functional groups or surface molecules. Owing to its distinct microscopic structure and physical chemistry properties, interfacial water displays behavior that differs significantly from that of bulk water. Consequently, investigations of interfacial water are important for developing a detailed understanding of water behavior near polymer surfaces and for enabling appropriate control of these interfacial properties.²

Interfacial water weakly associated with polymer surfaces is thought to contribute to the functional performance of biocompatible polymers.^{3,4} The scenario can be summarized as follows. Water molecules that are strongly associated with hydrophilic polymer surfaces can disrupt the hydration layer that stabilizes protein structure when proteins come into contact with the material. This disruption promotes protein denaturation and aggregation. Cells subsequently adhere to these

protein aggregates, eventually leading to thrombus formation. In contrast, polymers with high biocompatibility retain water molecules that are only weakly associated with the interface. These interfacial water molecules form a barrier that helps maintain the hydration layer of proteins at the polymer surface, thereby supporting biocompatible behavior.

A representative biocompatible polymer is polyethylene glycol (PEG), a water-soluble polymer synthesized from ethylene oxide.⁵ In addition to its high solubility in organic solvents, PEG exhibits low toxicity, chemical stability, and lubricity. Owing to its ability to suppress protein adsorption and cell adhesion, as well as its stable dispersion in aqueous media, PEG is widely employed in a range of applications. PEG-immobilized surfaces form highly hydrated layers in aqueous environments due to their strong affinity for water. The resulting hydration layer introduces an energetic barrier to protein adsorption, thereby inhibiting nonspecific protein binding.⁶

Poly(2-methoxyethyl acrylate) (PMEA) is a biocompatible polymer developed by Tanaka *et al.*⁷⁻⁹ PMEA exhibits properties including water insolubility, suppression of protein adsorption and denaturation, inhibition of platelet adhesion and activation, and low toxicity. Experimental research focusing on the hydration structure within PMEA have been conducted to clarify the mechanisms underlying its biocompatibility. In particular, differential scanning calorimetry (DSC) studies have reported that PMEA contains characteristic interfacial water.^{10,11} Interfacial water is commonly classified into three categories: free water, which freezes and melts at 0 °C; bound water, which remains nonfreezing even at -100 °C; and intermediate water, which undergoes crystallization and melt-

^{a)}Electronic mail: kk@cheng.es.osaka-u.ac.jp

^{b)}Electronic mail: nobuyuki@cheng.es.osaka-u.ac.jp

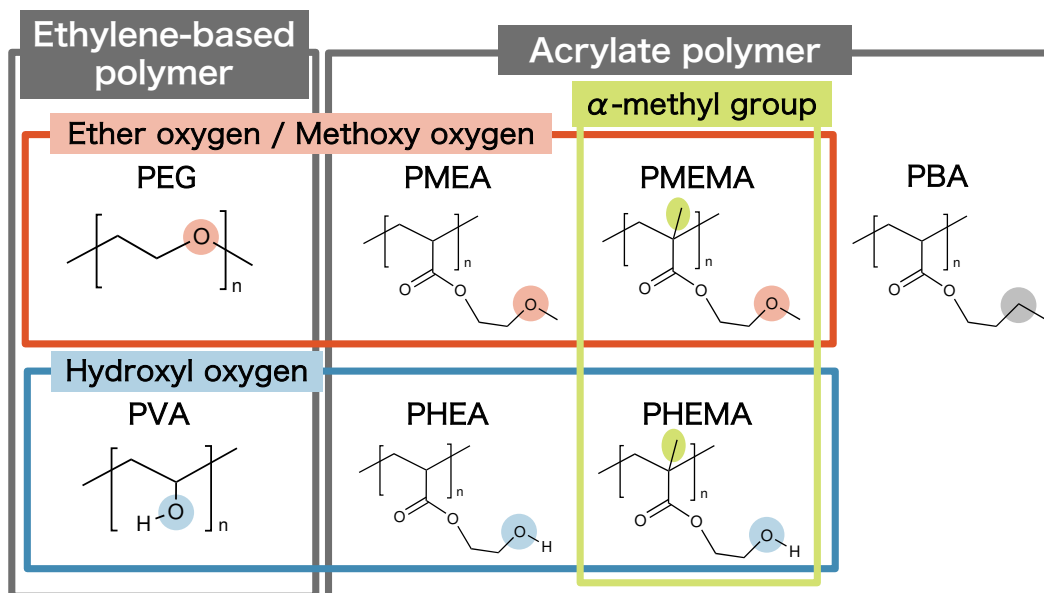


FIG. 1. Structure and classification of polymers studied in this paper.

ing at temperatures below the freezing point. Furthermore, evaluations of platelet adhesion indicate that the amount of intermediate water is a key factor governing the manifestation of antithrombotic effects. Note that PEG, the biocompatible polymer described above, has also been reported to contain intermediate water.¹²

The freezing and melting behavior of water observed by DSC provides important insights into the strength of interactions between polymers and water. Furthermore, low-temperature crystallization of water in the hydrated polymer was observed immediately after the glass transition during DSC heating.¹¹ This behavior suggests that the emergence of intermediate water is closely related to the glass transition temperature, T_g . When considering polymer properties, the glass transition temperature T_g is a critical parameter, and the expression of polymer functions depends strongly on the temperature difference between the ambient temperature and T_g . PEG and PMEA, both reported to contain intermediate water, exhibit glass transition temperatures T_g below 0 °C in the dry state. However, because the glass transition temperature T_g in the dry state does not describe water-polymer interactions, understanding molecular behavior in the vicinity of T_g under hydrated conditions is essential for elucidating the properties of polymers.

Molecular dynamics (MD) simulations provide a powerful approach for directly probing the local property of interfacial water in the vicinity of polymers. PEG, a hydrophilic polymer with a simple polyether backbone, has been extensively studied using MD simulations, with investigations addressing its polymer chain structure, hydration water content, H-bonds with water molecules, and glass transition behavior.^{13–28} Numerous MD simulations have also been performed on poly(vinyl alcohol) (PVA), a polymer with a structure similar to that of PEG and a representative gel-forming mate-

rial.^{29–46}

In addition, a number of MD studies have investigated the structural and dynamical characteristics of interface water confined within PMEA.^{47–64} Specifically, we performed MD simulations of PMEA and structurally related (meth)acrylate polymers, including poly(2-hydroxyethyl methacrylate) (PHEMA) and poly(1-methoxymethyl acrylate) (PMC1A), to elucidate the H-bond dynamics associated with each acceptor oxygen site for each polymer functional group.⁶¹ Our results indicate that, upon breakage of H-bonds between water molecules and the methoxy oxygen of PMEA, the water molecules remain in close proximity and do not diffuse on the picosecond timescale. In contrast, water molecules H-bonded to the hydroxy oxygen of PHEMA and the methoxy oxygen of PMC1A diffuse immediately following hydrogen-bond breakages.

In this study, we focus on the observation that not only PMEA but also PEG is a hydrophilic polymer exhibiting antithrombotic properties and intermediate water, and accordingly performed MD simulations. In addition, PVA, poly(2-hydroxyethyl acrylate) (PHEA), PHEMA, poly(2-methoxyethyl methacrylate) (PMEMA), and poly(butyl acrylate) (PBA) are simulated as negative controls. This MD analysis enables a comparative, comprehensive examination of ethylene-based polymers (PEG and PVA) and acrylate polymers (PMEA, PHEA, PMEMA, PHEMA, and PBA), allowing assessment of how variations in functional oxygen groups and the presence or absence of methyl side chains influence the behavior of water molecules in the vicinity of the polymers.

Figure 1 presents the chemical structures of the seven polymers examined. PEG contains an ether oxygen, whereas PMEA contains a carbonyl oxygen, an ether-like oxygen, and a methoxy oxygen. Replacement of the ether group with a hydroxyl group yields PVA and poly(2-hydroxyethyl acry-

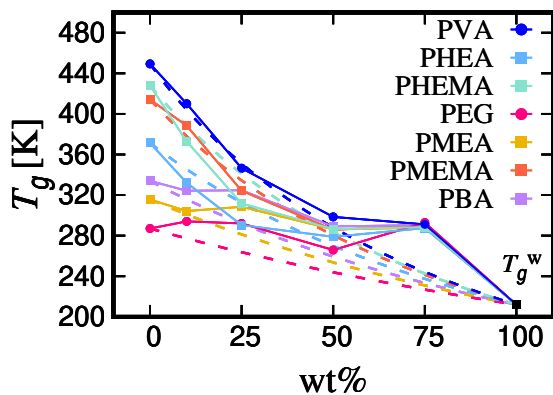


FIG. 2. Water content dependence of the glass transition temperature T_g . $T_g^w \approx 212$ K denotes the glass transition temperature of the TIP4P/2005 water model, as previously reported.⁶⁵ The dashed line represents the Fox equation [Eq. (1)], which estimates T_g for the water-polymer mixture system based on the glass transition temperatures of the dry polymer and pure water.

late) (PHEA), respectively. Introduction of an α -methyl side chain on the polymer backbone gives poly(2-methoxyethyl methacrylate) (PMEMA) and PHEMA, respectively, while replacement of the methoxy group in PMEA with an ethyl group results in poly(butyl acrylate) (PBA). The water solubility, equilibrium water content, glass transition temperature T_g in the dry state, blood compatibility, and presence or absence of intermediate water for these polymers are summarized in Table I of the Supplementary Material.

The analyses conducted in this study are summarized as follows. First, the glass transition temperature T_g under both dry and hydrated conditions was determined from the temperature dependence of the mass density. To assess the mobility of hydrated polymer chains, fluctuations in dihedral angle conformations were then examined. In addition, the H-bonding state of water molecules was characterized, and the associated time scales were quantified as H-bond lifetimes, with their temperature dependence analyzed. In combination, these analyses provide insight into water-polymer interactions. Finally, to clarify the mobility of water molecules confined within the polymers, the distinct part of van Hove correlation function, which describes molecular exchange processes among water molecules, was evaluated.

II. SIMULATION DETAILS

Each polymer was modeled using J-OCTA⁶⁶ with the OPLS-AA force field.⁶⁷ The polymer chains were constructed as atactic with a 1:1 stereoregularity and a degree of polymerization of 50. Additionally, quantum chemistry calculations were performed to determine atomic charges at a degree of oligomerization of 11 with the same form of tacticity, following the protocol described in Ref. 68. H atoms were added to both polymer terminal, and the number of polymer molecules in the simulation box was set to 20. Water molecules were

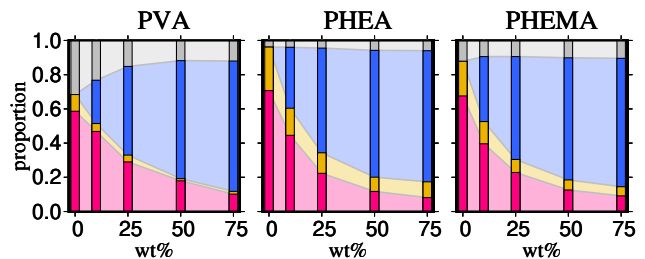


FIG. 3. Proportions of H-bonding partners for hydroxyl oxygen atoms in PVA, PHEA, and PHEMA at 300 K. Magenta denotes intermolecular H-bonds to oxygen acceptors on other polymer chains; yellow denotes intramolecular H-bonds to oxygen atoms on the same polymer chain; blue denotes H-bonds to oxygen atoms of water molecules; gray denotes hydroxyl oxygen atoms that do not participate in H-bonding.

represented by the TIP4P/2005 model⁶⁹ and added to the systems under periodic boundary conditions to achieve the mass water contents of 0, 10, 25, 50, and 75 wt%. MD simulations were carried out using GROMACS 2024.4,⁷⁰ and the initial configurations were generated with PACKMOL.⁷¹

After energy minimization, system equilibration was performed in a manner similar to that described in Ref. 68, with details provided in Table II of the Supplementary Material. *NVT* simulations employed the velocity-rescaling method for temperature control.⁷² In *NPT* simulations, temperature control was also achieved using velocity rescaling, while pressure was regulated using the stochastic cell-rescaling method.⁷³ In all MD simulations, the time step was set to 1 fs.

III. RESULTS AND DISCUSSION

A. Glass transition temperature

To examine the temperature dependence of the mass density ρ , MD simulations were conducted during a cooling protocol. After equilibration at 600 K (for 0 wt% and 10 wt% systems of PVA, PHEA, PMEMA, and PHEMA) or 500 K (for the other systems), the temperature was reduced stepwise by 20 K, and at each temperature, *NPT* simulations of 4.05 ns followed by *NVT* simulations of 10 ns were performed. Figure S1 of the Supplementary Material presents the temperature dependence of ρ for each polymer at different water contents. It also presents the temperature dependence of the mass density of pure water described by the TIP4P/2005 model using a system of 1000 molecules. For the pure water system, the temperature dependence of the mass density exhibits non-monotonic behavior, with a maximum at approximately 280 K followed by an increase at lower temperatures, as shown in Fig. S1 of the Supplementary Material. This behavior reflects the presence of two liquid states of water, namely, a high-density liquid and a low-density liquid.^{74–76} Kreck *et al.* characterized the glass transition temperature T_g of various water models by calculating heat capacity using MD simulations, reporting $T_g \approx 212$ K for the TIP4P/2005 model.⁶⁵

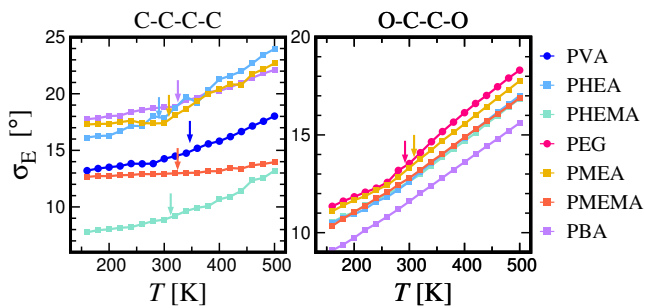


FIG. 4. Temperature dependence of σ_E , which quantifies the spread of the Gaussian mixture model distribution, at a water content of 25 wt%. The left panel shows the main-chain carbon dihedral angle (C-C-C-C), and the right panel shows the carbon skeleton dihedral angle associated with the oxygen substituent (O-C-C-O). For PBA, the latter corresponds to the O-C-C-C dihedral angle that includes the butyl group. The arrows indicate the glass transition temperature T_g for for PEG and PMEA in the panel for O-C-C-O and for the others in the panel for C-C-C-C.

At a water content of 0 wt% in the dry state, polymers containing hydroxyl groups exhibit higher densities than those containing ether groups, consistent with experimental tendency. Furthermore, the density decreases with increasing water content for each polymer. As the temperature decreases, a change in slope is observed at a characteristic temperature, which defines the glass transition temperature T_g . A common approach for estimating the glass transition temperature T_g is to approximate the density-temperature dependence with two linear fits and determine T_g from their intersection. Figure S1 of the Supplementary Material shows these linear fits for each polymer at water contents below 25 wt%. However, at water contents above 50 wt%, the non-monotonic behavior in density-temperature curve was observed, reflecting the anomalous temperature dependent of pure water, as noted above. In this regime, linear fitting becomes difficult; therefore, T_g is defined as the temperature at which the second derivative of ρ with respect to temperature attains a minimum. For this purpose, the Savitzky–Golay filter was applied to perform second-order differentiation of the density-temperature data.⁷⁷ The resulting T_g determined from the minimum of the second derivative of ρ with respect to T is shown in Fig. S1 of the Supplementary Material.

Figure 2 shows the glass transition temperature T_g as a function of the water content for the seven polymer systems. For reference, an empirical relation based on the Fox equation for estimating the glass transition temperature of a binary mixture is also shown. The Fox equation assumes equal free-volume fractions for components 1 and 2 and is expressed as

$$\frac{1}{T_g} = \frac{w_1}{T_{g,1}} + \frac{w_2}{T_{g,2}}, \quad (1)$$

where w_1 and w_2 are the weight fractions of component 1 and 2, respectively and $T_{g,1}$ and $T_{g,2}$ denote the corresponding glass transition temperatures.⁷⁸

In the dry state (0 wt%), MD simulations reproduced consistent trends in the glass transition temperatures. However,

owing to the high cooling rates employed in the simulations, the calculated T_g values are approximately 40–120 K higher than the experimental values. A study by Soldera and Metatla proposed a method for correcting T_g values obtained from MD simulations using the Williams–Landel–Ferry (WLF) equation,

$$\Delta T_g = \frac{-B \log_{10} \frac{q_{\text{sim}}}{q_{\text{exp}}}}{A + \log_{10} \frac{q_{\text{sim}}}{q_{\text{exp}}}}, \quad (2)$$

where ΔT_g represents the difference in T_g between cooling rates q_{sim} in MD simulations and q_{exp} in experiments.⁷⁹ Furthermore, the constants $A = 16.7$ and $B = 48$ K are fitting parameters determined as average values for some polymer systems. Figure S2 of the Supplementary Material shows the relationship between the corrected T_g values from MD simulations and the experimental values. This indicates that the corrected T_g is consistent with experimentally reported values, within a deviation of approximately 40 K. Note that PMEMA shows the largest overestimation from the experimental values by the MD simulations. Nevertheless, of the seven polymers examined, PVA, PHEA, and PHEMA exhibit relatively higher T_g values in the dry state, consistent with experimental observations. This behavior is attributed to the formation of intermolecular H-bonds mediated by hydroxyl groups and to increased chain rigidity arising from α -methyl side chains along the polymer backbone.

However, because experimental T_g values under water-saturated conditions are limited, the following discussion is based on uncorrected T_g values without applying the WLF equation. Figure 2 demonstrates that with addition of water, T_g reduces from that at the dry state, with this trend being particularly pronounced for polymers with high dry-state T_g . This behavior arises from water-induced plasticization of the polymer matrix.⁸⁰ Indeed, a pronounced decrease in the glass transition temperature with increasing water content has been experimentally observed for PVA,^{81,82} PHEA,⁸³ and PHEMA.^{84–86} Furthermore, although the Fox equation captures the overall trend, it underestimates the magnitude of the plasticizing effect, particularly for PHEA and PHEMA. This suggests that hydroxyl groups in PHEA and PHEMA contribute to plasticization not only through H-bond formation between polymer chains but also via H-bonding between the polymer and water molecules.

To elucidate the plasticization effect of water molecules, particularly for PVA, PMEA, and PHEMA, we analyzed in detail the water content dependence of the probability distribution of H-bonding partners associated with hydroxyl oxygen atoms. Here, H-bond between donor and acceptor was defined when the oxygen-oxygen distance r_{OO} was 0.35 nm or less and the oxygen \cdots oxygen-hydrogen angle was 30° or less.^{87–89} The results obtained at a temperature of 300 K are shown in Fig. 3. In the dry state, approximately 90% of the hydroxyl oxygen atoms in PHEA and PHEMA participate in H-bonding, and this fraction remains essentially unchanged upon hydration. As the water content increased, the fractions of intermolecular and intramolecular H-bonds decreased, while the proportion of H-bonds formed with water molecules increased. Accordingly, in PHEA and PHEMA, the hydroxyl

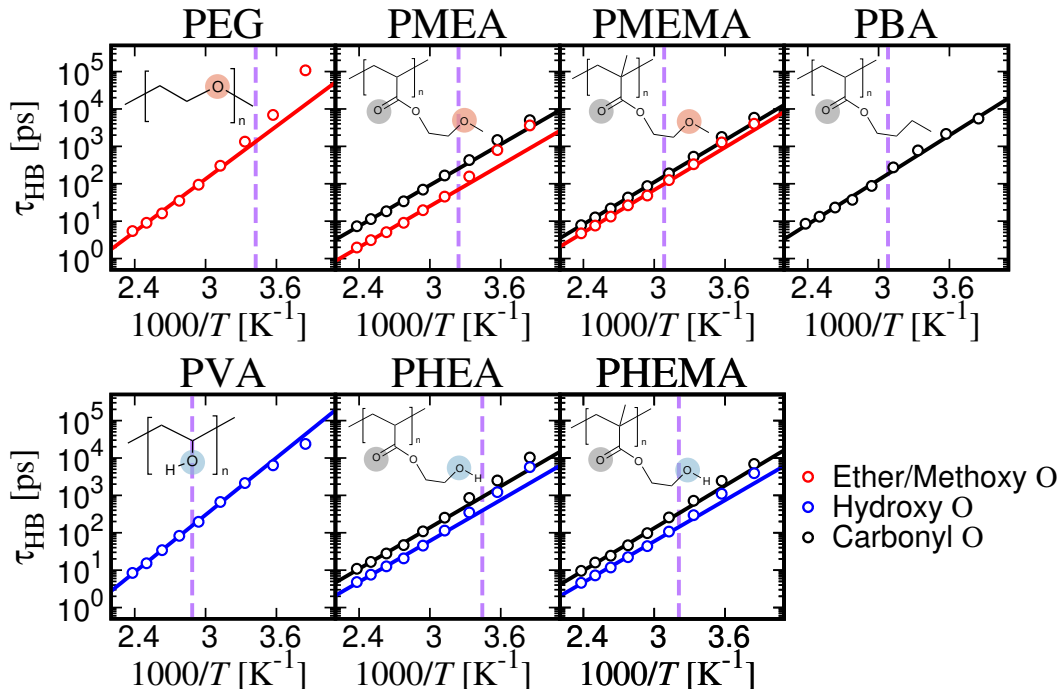


FIG. 5. Arrhenius plots of τ_{HB} between water molecules and acceptor oxygens of polymer functional groups at a water content of 25 wt% (260–420 K in 20 K intervals). Red symbols denote H-bonds with ether or methoxy oxygens, red symbols correspond to hydroxyl oxygens, and black symbols represent carbonyl oxygens in acrylate groups as acceptors. The solid lines indicate linear fits in the high-temperature range (340–420 K). The purple dashed line represents the estimated glass transition temperature T_g .

oxygen atoms in the acrylate side chains readily exchange their H-bonding partners from polymers to nearby water molecules, resulting in a pronounced plasticization effect. In contrast, PVA contains a relatively large fraction of hydroxyl oxygen atoms that do not participate in H-bonding in the dry state owing to its short side-chain structure. Although the proportion of H-bonds formed with water molecules increases gradually upon hydration, this fraction remains smaller than those of PHEA and PHEMA up to a water content of 25 wt%, indicating a weaker plasticization effect.

As the dry-state T_g decreases, the dependence of T_g on water content becomes weaker, indicating a limited plasticization effect. This trend is particularly evident for PEG, for which T_g exhibits little change with increasing water content, in agreement with experimental observations.^{12,90–92} Interestingly, the water content dependence of the glass transition temperatures T_g for the seven polymers with markedly different dry-state T_g values, shown in Fig. 2, is consistent with experimental findings that, in polyol liquids, the number of H-bondable hydroxyl groups correlates with T_g in aqueous environments.^{93,94} When the water content exceeds 50 wt% and water becomes excessive in the system, T_g converges to a nearly constant value of approximately 280 K, as shown in Fig. 2. This behavior can be interpreted as water becoming the dominant component, thereby diminishing the distinct characteristics of each polymer. It should be noted, however,

that water contents of 50 wt% or higher represent virtual conditions in the MD simulations and do not correspond to the water contents of real systems.

B. Fluctuations in dihedral angles

Section III A demonstrated that the glass transition temperature T_g exhibits significant changes in its water content dependence due to differences in side chains and functional groups. Recently, Jin *et al.* reported that fluctuations of dihedral angles in polymer melts, including both main-chain and side-chain degrees of freedom, correlate with T_g .^{95,96} Building on these studies, we quantified dihedral angle fluctuations associated with the conformations of polymer chains and examine their relationship with T_g . Here, we analyzed dihedral angles defined by the main chain carbon atoms (C-C-C-C) as well as those involving oxygen substituents (O-C-C-O) at the polymer terminal, as exemplified by PEG and PMEa. Note that, in the case of PBA, the O-C-C-C dihedral angle, containing the butyl group, is considered instead.

Figure S3 of the Supplementary Material shows the distributions of the dihedral angles for C-C-C-C and O-C-C-O at the water content of 25 wt%. Similar overall trends were obtained at 10 wt% and 50 wt% and at other temperatures; however, the peak height decreases with increasing temperature

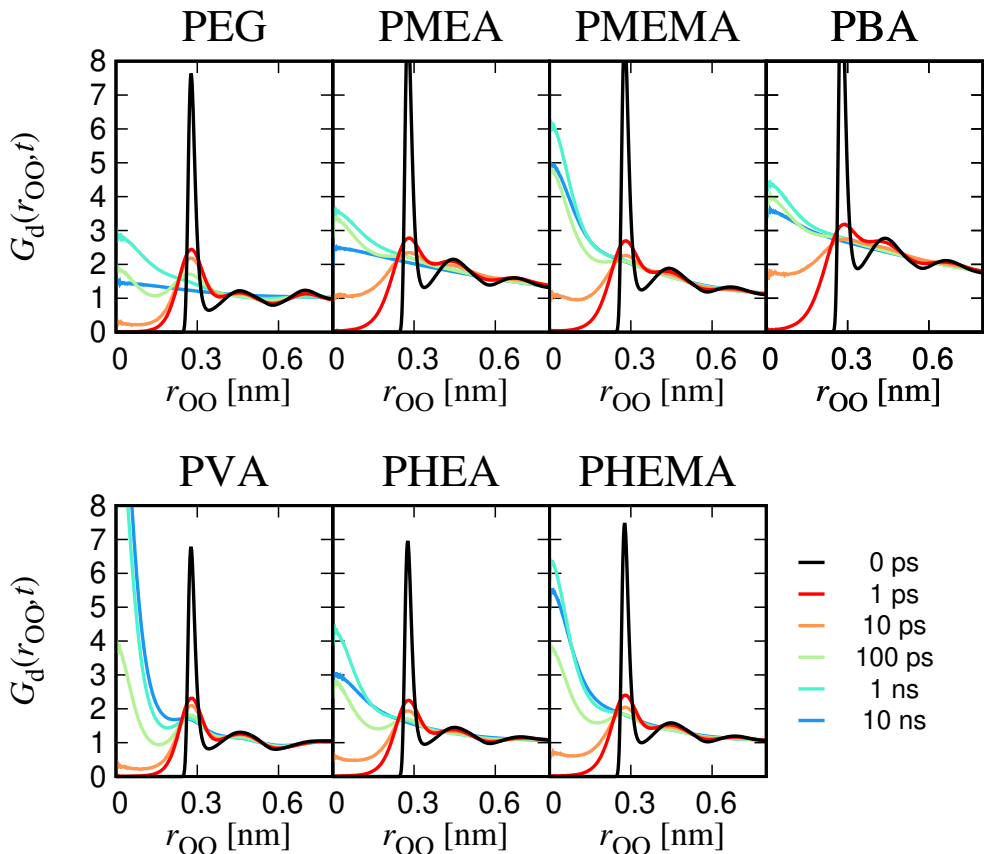


FIG. 6. Distinct part of the van Hove correlation function, $G_d(r_{OO}, t)$, for the oxygen-oxygen distance between water molecules at a water content of 25 wt% and a temperature of 300 K. The black curve ($t = 0$ ps) corresponds to the radial distribution function between oxygen atoms.

and water content (data not shown). For each polymer, the distributions exhibit peaks corresponding to the gauche configuration (60° and 300°) and the trans configuration (180°). Notably, the O-C-C-O dihedral angles of PEG, PMEAs, and PHEMA predominantly adopt the gauche conformation, indicating enhanced chain flexibility. Following the same algorithm described in Ref. 95, we employed a Gaussian mixture model that represents the data as a superposition of Gaussian distributions. Specifically, we approximated the distribution as a mixture of three Gaussian components centered at the trans ($\approx 180^\circ$), gauche- ($\approx 60^\circ$), and gauche+ ($\approx 300^\circ$) angles, and extracted the corresponding center positions and standard deviations. The results are also shown in Fig. S3 of the Supplementary Material. The mixture proportion w_i and standard deviation σ_i of the i -th Gaussian distribution were used to define the magnitude of the dihedral angle fluctuation as $\sigma_E = \sum_{i=1}^3 w_i \sigma_i$. The magnitude of σ_E quantifies the overall spread of the dihedral angle distribution, and is therefore expected to correlate with the extent of structural fluctuations within a given conformation as well as the propensity for tran-

sitions between different conformations.

The temperature dependence of σ_E of C-C-C-C and O-C-C-O angles for each polymer at 25 wt% is plotted in Fig. 4. As seen in the figure, σ_E decreases with decreasing temperature. The magnitude of σ_E for C-C-C-C dihedral angle is relatively large for PMEAs, PHEAs, and PBA, and smaller for PMEMAs and PHEMA, which contain α -methyl side group on the main chain. PVA exhibits intermediate behavior. These results indicate that α -methyl side groups along the backbone reduce overall chain mobility. Furthermore, the temperature dependence of σ_E becomes more gradual near and below the glass transition temperature, T_g , consistent with previously reported findings.⁹⁶

Figure 4 also shows that the magnitude of σ_E for O-C-C-C dihedral angle decreases in the order PEG > PMEAs > PHEAs > PHEMA > PMEMAs > PBA. In addition, PEG and PMEAs exhibit a change in slope near T_g , analogous to that observed for the C-C-C-C dihedral angle. PEG and PMEAs exhibit greater mobility compared to other polymers, suggesting that the rotational freedom of their ether groups results

in less steric constraint. In contrast, in the other polymers, dihedral angle fluctuations are reduced by steric constraints imposed by α -methyl side chains and by H-bonding involving hydroxyl oxygen atoms. Note that the smallest value of σ_E observed for PBA originates from fluctuations in the O-C-C-C dihedral angle. Compared with the O-C-C-O linkage, this behavior can be attributed to the larger steric size and lower rotational freedom of the butyl group, which restricts conformational flexibility.

C. H-Bond lifetime

This subsection examines the dynamic behavior of water molecules in the vicinity of the polymers. For this purpose, we analyzed the H-bond time correlation function, $P_{\text{HB}}(t)$, using 10 ns trajectories in the NVT ensemble over the temperature range 260 to 420 K at 20 K intervals. Specifically, $P_{\text{HB}}(t)$ represents the probability that an H-bond remains intact at time t , given that a specific donor-acceptor pair is H-bonded at $t = 0$.^{87–89,97} It is given as

$$P_{\text{HB}}(t) = \frac{\langle h_{i,j}(t)h_{i,j}(0) \rangle}{\langle h_{i,j}(0) \rangle}, \quad (3)$$

where $h_{i,j}(t)$ is the H-bond indicator function, which takes a value of unity if water molecule i (acting as the donor) and the acceptor oxygen j belonging to a polymer functional group are H-bonded at time t , and zero otherwise. $\langle \dots \rangle$ represents the ensemble average over all possible pairs of H-bonds at the initial time 0. The calculated $P_{\text{HB}}(t)$ is shown in Fig. S4 of the Supplementary Material. Note that $P_{\text{HB}}(t)$ at 300 K for PMEAs and PHEMA was reported in Ref. 61. $P_{\text{HB}}(t)$ was fitted by the Kohlrausch–Williams–Watts (KWW) function, $P_{\text{HB}}(t) \approx \exp[-(t/\tau_{\text{KWW}})^{\beta_{\text{KWW}}}]$. The integral of $P_{\text{HB}}(t)$ characterizes the H-bond lifetime τ_{HB} ,

$$\tau_{\text{HB}} = \int_0^{\infty} P_{\text{HB}}(t) dt, \quad (4)$$

yielding an estimation of $\tau_{\text{HB}} = (\tau_{\text{KWW}}/\beta_{\text{KWW}})\Gamma(1/\beta_{\text{KWW}})$ using the Gamma function $\Gamma(\cdot)$.

Figure 5 presents the Arrhenius plot of τ_{HB} as a function of inverse temperature for each acceptor oxygen associated with the polymer functional groups at a water content of 25 wt%. As H-bond acceptors in the polymer functional groups, ether oxygen, methoxy oxygen, hydroxyl oxygen, and carbonyl oxygen were considered. Here, ether-like oxygen atoms adjacent to carbonyl groups were excluded from the analysis because their contribution to H-bond is negligible due to the influence of the carbonyl group.⁶¹ The linear fit in the Arrhenius plot corresponds to the activation energy associated with H-bond breakages. At temperatures below the glass transition temperature T_g , a pronounced increase in τ_{HB} is observed for both the ether oxygen in PEG and the methoxy oxygen in PMEAs, deviating from Arrhenius behavior observed in the higher temperature regime. In contrast, for polymer functional groups other than the ether oxygen in PEG and the

methoxy oxygen in PMEAs, τ_{HB} exhibits an approximately Arrhenius temperature dependence. These results suggest that the strength of H-bonding between water molecules and the ether oxygen in PEG and the methoxy oxygen in PMEAs varies with temperature. In other words, above T_g the H-bonds are relatively weak and transient, whereas below T_g they become more stable and longer-lived. For example, when comparing the methoxy oxygen in PMEAs with those in PHEA, PMEMA, and PHEMA, τ_{HB} for PMEAs is smaller at high temperatures; however, at $T = 240$ K, below T_g , the values of τ_{HB} become comparable.

IV. WATER MOLECULE EXCHANGE DYNAMICS

Differences among functional group oxygens that form H-bonds with the polymer are expected to influence the mobility of the associated water molecules, particularly the exchange of positions between neighboring water molecules. To clarify this aspect, we analyzed the water molecule exchange dynamics via van Hover correlation function, specifically its distinct part, $G_d(r_{\text{OO}}, t)$, defined in terms of the oxygen-oxygen distance r_{OO} between two distinct water molecules.⁹⁸ Figure 6 shows the results for $G_d(r_{\text{OO}}, t)$ at a water content of 25 wt% for each polymer.

As structural relaxation proceeds, the information on the initial intermolecular configuration is lost; accordingly, $G_d(r_{\text{OO}}, t)$ is expected to approach unity at all r_{OO} in the long-time limit. Indeed, for all polymers, the peak in $G_d(r_{\text{OO}}, t)$ corresponding to the first hydration shell decreases progressively with time. However, an increase in $G_d(r_{\text{OO}}, t)$ is observed in the vicinity of $r_{\text{OO}} = 0$, a feature that has also been reported for hydrated PVA systems.³⁴ This behavior indicates the hopping motion of water molecules from the first hydration shell toward the origin, reflecting water-water exchange processes arising from the localization of water molecules confined within the polymer matrix. As shown in Fig. 6, this feature is particularly pronounced for PVA, PHEA, PMEMA, PHEMA, and PBA compared with PEG and PMEAs. PVA, PHEA, and PHEMA are hydrophilic polymers containing hydroxyl groups and exhibit relatively long H-bond lifetimes with water, indicating a strong confinement effect on the associated water molecules. In contrast, PMEMA and PBA are more hydrophobic and possess lower equilibrium water contents, with a tendency for polymer chain aggregation. Consequently, water molecules spatially confined within such polymer matrices are expected to become localized. By comparison, PEG and PMEAs possess flexible backbones derived from ether and methoxy groups, respectively, as demonstrated in Fig. 4. This flexibility enhances the mobility of confined water molecules, resulting in a reduced localization effect as characterized by $G_d(r_{\text{OO}}, t)$.

V. CONCLUSIONS

In this study, we performed MD simulations to systematically investigate seven hydrated polymers, encompassing

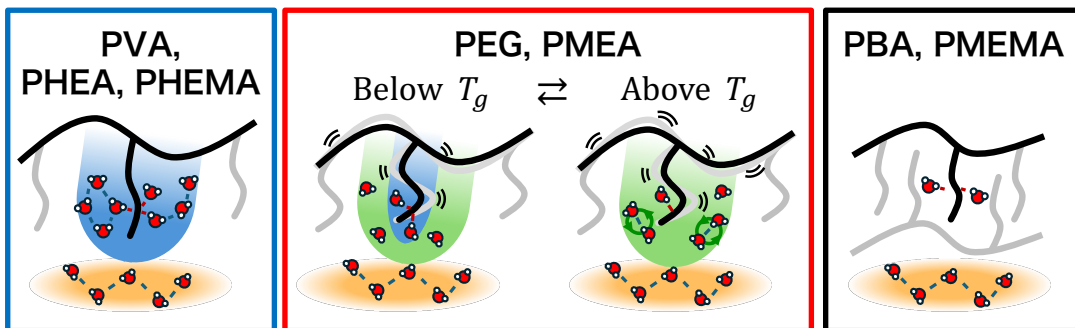


FIG. 7. Schematic illustration of the states of interfacial water in the vicinity of polymers. Hydrated type (PVA, PHEA, PHEMA): Low polymer chain mobility and strong H-bonding lead to the formation of a localized hydration shell, in which water molecules are tightly confined. Flexibly hydrated type (PEG, PMEAs): Below T_g , restricted polymer mobility results in strongly bound water H-bonded with ether or methoxy oxygen atoms, which exhibits dynamically distinct behavior from the surrounding, more mobile (loosely bound) water. Above T_g , enhanced polymer mobility gives rise to a predominance of loosely bound water in the vicinity of the polymers. Hydrophobic type (PBA, PMEMA): Hydrophobic interactions induce aggregations of the polymers. The system is partitioned into polymer-bound water and bulk-like water.

ethylene-based and acrylate polymers. Specifically, we elucidated the behavior of interfacial water in each polymer from four perspectives: (i) the water-content dependence of the glass transition temperature, (ii) polymer chain fluctuations characterized by dihedral angle distributions, (iii) H-bond lifetimes between water molecules and polymer functional groups, and (iv) the exchange dynamics of water molecules confined within the polymer matrix.

Based on these analyses, the seven polymers can be broadly classified into three groups. The first group consists of hydrophilic polymers containing hydroxyl groups, namely PVA, PHEA, and PHEMA. These polymers exhibit relatively high glass transition temperatures T_g in the dry state and a pronounced decrease in T_g with increasing water content. Their polymer chain fluctuations are small, and the H-bond lifetimes τ_{HB} between hydroxyl oxygen atoms and water molecules follow Arrhenius behavior. The second group comprises PBA and PMEMA, which are characterized by low equilibrium water contents and hydrophobic properties. Their dry-state T_g values are slightly lower than those of the hydrophilic polymers, and the reduction in T_g upon hydration is less pronounced. Similar to the first group, however, they exhibit limited chain fluctuations, and τ_{HB} also obeys Arrhenius behavior. The third group consists of PEG and PMEAs, which contain ether and methoxy groups, respectively. These polymers exhibit relatively low glass transition temperatures T_g in the dry state, and the influence of water content on T_g is modest. Owing to the rotational freedom of the ether and methoxy oxygen atoms, polymer chain fluctuations are comparatively large. In addition, the H-bond lifetimes τ_{HB} display super-Arrhenius behavior below T_g .

Furthermore, in conjunction with the localization effect of water molecules confined within the polymer matrix, as characterized by the van Hove correlation function, $G_d(r_{OO}, t)$, the interfacial water surrounding the polymers can be classified according to the hydration mechanism into three categories: highly hydrated (PVA, PHEA, and PHEMA), hydrophobic (PMEMA and PBA), and flexibly hydrated (PEG and PMEAs)

types. A schematic illustration of this conceptual framework is presented in Fig. 7. For the highly hydrated type, each polymer chain maintains a stable structure and forms a localized hydration shell through H-bonding mediated by hydroxyl oxygen atoms. For the hydrophobic type, the tendency of polymer chains to aggregate due to hydrophobic interactions leads to a localization of H-bonded water molecules. For the flexibly hydrated type (PEG and PMEAs), the polymer chains exhibit high mobility owing to the presence of ether or methoxy oxygen atoms, suggesting that water molecules H-bonded to these sites are only loosely bound. However, below T_g , the activation energy associated with H-bond dissociation increases, indicating the formation of stronger H-bonds under glassy conditions. Although a direct correspondence with DSC measurements is not straightforward, a consistent interpretation can be proposed for PEG and PMEAs as follows. Below T_g , water molecules located in the vicinity of ether or methoxy oxygen atoms are constrained within the glassy polymer matrix. Upon heating above T_g , the recovery of polymer chain mobility enhances the diffusivity of these water molecules, enabling their transition to a diffusion-dominated regime. If this process leads to low-temperature crystallization during the heating scan, it provides a picture that is consistent with the concept of intermediate water.

SUPPLEMENTARY MATERIAL

The supplementary material provides the experimental properties of the seven polymers (Table SI), the system equilibration protocol (Table SII), the temperature dependence of mass density (Fig. S1), relationship between the corrected glass transition temperature and the experimental values (Fig. S2), distributions of the dihedral angles (Fig. S3), and the H-bond correlation function $P_{HB}(t)$ (Fig. S4).

ACKNOWLEDGMENTS

The authors thank Hidekazu Kojima for helpful comments. This work was supported by JSPS KAKENHI Grant-in-Aid Grant Nos. JP25KJ1764, JP25K00968, JP24H01719, JP22H04542, JP22K03550, and JP23H02622. We acknowledge support from the Fugaku Supercomputing Project (Nos. JPMXP1020230325 and JPMXP1020230327) and the Data-Driven Material Research Project (No. JPMXP1122714694) from the Ministry of Education, Culture, Sports, Science, and Technology and by Maruho Collaborative Project for Theoretical Pharmaceutics. The numerical calculations were performed at Research Center of Computational Science, Okazaki Research Facilities, National Institutes of Natural Sciences (Projects: 25-IMS-C052).

AUTHOR DECLARATIONS

CONFLICT OF INTEREST

The authors have no conflicts to disclose.

DATA AVAILABILITY STATEMENT

The data that support the findings of this study are available from the corresponding author upon request.

- ¹N. Bayliss and B. V. K. J. Schmidt, “Hydrophilic polymers: Current trends and visions for the future,” *Prog. Polym. Sci.* **147**, 101753 (2023).
- ²X. Wan, M. Liu, F. Zhang, L.-P. Xu, and S. Wang, “Interfacial Chemistry in Functional Hydrogel Coatings,” *Angew. Chem. Int. Ed.* **64**, e202425552 (2025).
- ³T. Tsuruta, “On the Role of Water Molecules in the Interface between Biological Systems and Polymers,” *J. Biomater. Sci. Polym. Ed.* **21**, 1831–1848 (2010).
- ⁴M. Tanaka, S. Morita, and T. Hayashi, “Interfacial water states and the biocompatibility of biomaterials: The role of intermediate water,” *Polym. J.* , 1–14 (2026).
- ⁵J. M. Harris, ed., *Poly(Ethylene Glycol) Chemistry: Biotechnical and Biomedical Applications* (Springer, Boston, MA, 1992).
- ⁶S. I. Jeon, J. H. Lee, J. D. Andrade, and P. G. De Gennes, “Protein—surface interactions in the presence of polyethylene oxide: I. Simplified theory,” *J. Colloid Interface Sci.* **142**, 149–158 (1991).
- ⁷M. Tanaka, T. Motomura, N. Ishii, K. Shimura, M. Onishi, A. Mochizuki, and T. Hatakeyama, “Cold crystallization of water in hydrated poly(2-methoxyethyl acrylate) (PMEA),” *Polym. Int.* **49**, 1709–1713 (2000).
- ⁸M. Tanaka, T. Motomura, M. Kawada, T. Anzai, Yuu Kasori, T. Shiroya, K. Shimura, M. Onishi, and Akira Mochizuki, “Blood compatible aspects of poly(2-methoxyethylacrylate) (PMEA)—relationship between protein adsorption and platelet adhesion on PMEA surface,” *Biomaterials* **21**, 1471–1481 (2000).
- ⁹M. Tanaka and A. Mochizuki, “Effect of water structure on blood compatibility— thermal analysis of water in poly(meth)acrylate,” *J. Biomed. Mater. Res. A* **68A**, 684–695 (2004).
- ¹⁰M. Tanaka, K. Sato, E. Kitakami, S. Kobayashi, T. Hoshiba, and K. Fukushima, “Design of biocompatible and biodegradable polymers based on intermediate water concept,” *Polym. J.* **47**, 114–121 (2015).
- ¹¹K. Sato, S. Kobayashi, M. Kusakari, S. Watahiki, M. Oikawa, T. Hoshiba, and M. Tanaka, “The Relationship Between Water Structure and Blood Compatibility in Poly(2-methoxyethyl Acrylate) (PMEA) Analogues: The Relationship Between Water Structure and Blood Compatibility...” *Macromol. Biosci.* **15**, 1296–1303 (2015).
- ¹²T. Hatakeyma, H. Kasuga, M. Tanaka, and H. Hatakeyama, “Cold crystallization of poly(ethylene glycol)—water systems,” *Thermochim. Acta* **465**, 59–66 (2007).
- ¹³G. D. Smith, R. L. Jaffe, and D. Y. Yoon, “Force field for simulations of 1,2-dimethoxyethane and poly(oxyethylene) based upon ab initio electronic structure calculations on model molecules,” *J. Phys. Chem.* **97**, 12752–12759 (1993).
- ¹⁴G. D. Smith, D. Bedrov, and O. Borodin, “Molecular Dynamics Simulation Study of Hydrogen Bonding in Aqueous Poly(Ethylene Oxide) Solutions,” *Phys. Rev. Lett.* **85**, 5583–5586 (2000).
- ¹⁵K. Tasaki, “Poly(oxyethylene)-Water Interactions: A Molecular Dynamics Study,” *J. Am. Chem. Soc.* **118**, 8459–8469 (1996).
- ¹⁶K. Tasaki, “Poly(oxyethylene)—cation interactions in aqueous solution: A molecular dynamics study,” *Comput. Theor. Polym. Sci.* **9**, 271–284 (1999).
- ¹⁷O. Borodin, D. Bedrov, and G. D. Smith, “A Molecular Dynamics Simulation Study of Polymer Dynamics in Aqueous Poly(ethylene oxide) Solutions,” *Macromolecules* **34**, 5687–5693 (2001).
- ¹⁸O. Borodin, D. Bedrov, and G. D. Smith, “Concentration Dependence of Water Dynamics in Poly(Ethylene Oxide)/Water Solutions from Molecular Dynamics Simulations,” *J. Phys. Chem. B* **106**, 5194–5199 (2002).
- ¹⁹E. E. Dormidontova, “Role of Competitive PEO-Water and Water-Water Hydrogen Bonding in Aqueous Solution PEO Behavior,” *Macromolecules* **35**, 987–1001 (2002).
- ²⁰A. Juneja, J. Numata, L. Nilsson, and E. W. Knapp, “Merging Implicit with Explicit Solvent Simulations: Polyethylene Glycol,” *J. Chem. Theory Comput.* **6**, 1871–1883 (2010).
- ²¹C. Wu, “Simulated Glass Transition of Poly(ethylene oxide) Bulk and Film: A Comparative Study,” *J. Phys. Chem. B* **115**, 11044–11052 (2011).
- ²²P. F. J. Fuchs, H. S. Hansen, P. H. Hünenberger, and B. A. C. Horta, “A GROMOS Parameter Set for Vicinal Diether Functions: Properties of Polyethyleneoxide and Polyethyleneglycol,” *J. Chem. Theory Comput.* **8**, 3943–3963 (2012).
- ²³C. Wu, “Glass transition in single poly(ethylene oxide) chain: A molecular dynamics simulation study,” *J. Polym. Sci. B Polym. Phys.* **55**, 178–188 (2017).
- ²⁴D. Sponseller and E. Blaisten-Barojas, “Solutions and Condensed Phases of PEG₂₀₀₀ from All-Atom Molecular Dynamics,” *J. Phys. Chem. B* **125**, 12892–12901 (2021).
- ²⁵M. Klajmon, V. Aulich, J. Ludfík, and C. Červinka, “Glass Transition and Structure of Organic Polymers from All-Atom Molecular Simulations,” *Ind. Eng. Chem. Res.* **62**, 21437–21448 (2023).
- ²⁶M. M. Hoffmann, M. D. Too, N. A. Paddock, R. Horstmann, S. Kloth, M. Vogel, and G. Buntkowsky, “On the Behavior of the Ethylene Glycol Components of Polydisperse Polyethylene Glycol PEG200,” *J. Phys. Chem. B* **127**, 1178–1196 (2023).
- ²⁷T. H. Ho, T. D. Hien, Ø. Wilhelmsen, and T. T. Trinh, “Thermophysical properties of polyethylene glycol oligomers *via* molecular dynamics simulations,” *RSC Adv.* **14**, 28125–28137 (2024).
- ²⁸H. Gudla and C. Zhang, “How to Determine Glass Transition Temperature of Polymer Electrolytes from Molecular Dynamics Simulations,” *J. Phys. Chem. B* **128**, 10537–10540 (2024).
- ²⁹Y. Tamai, H. Tanaka, and K. Nakanishi, “Molecular Dynamics Study of Polymer-Water Interaction in Hydrogels. 2. Hydrogen-Bond Dynamics,” *Macromolecules* **29**, 6761–6769 (1996).
- ³⁰Y. Tamai, H. Tanaka, and K. Nakanishi, “Molecular Dynamics Study of Polymer-Water Interaction in Hydrogels. 1. Hydrogen-Bond Structure,” *Macromolecules* **29**, 6750–6760 (1996).
- ³¹Y. Tamai, H. Tanaka, and K. Nakanishi, “Molecular Dynamics Study of Water in Hydrogels,” *Mol. Simul.* **16**, 359–374 (1996).
- ³²F. Müller-Plathe and W. F. van Gunsteren, “Solvation of poly(vinyl alcohol) in water, ethanol and an equimolar water-ethanol mixture: Structure and dynamics studied by molecular dynamics simulation,” *Polymer* **38**, 2259–2268 (1997).
- ³³F. Müller-Plathe, “Different States of Water in Hydrogels?” *Macromolecules* **31**, 6721–6723 (1998).
- ³⁴F. Müller-Plathe, “Microscopic dynamics in water-swollen poly(vinyl alcohol),” *J. Chem. Phys.* **108**, 8252–8263 (1998).

- ³⁵F. Müller-Plathe, "Diffusion of water in swollen poly(vinyl alcohol) membranes studied by molecular dynamics simulation," *J. Membr. Sci.* **141**, 147–154 (1998).
- ³⁶Y. Tamai and H. Tanaka, "Dynamic properties of supercooled water in poly(vinyl alcohol) hydrogel," *Chem. Phys. Lett.* **285**, 127–132 (1998).
- ³⁷Y. Tamai and H. Tanaka, "Effects of polymer chains on structure and dynamics of supercooled water in poly(vinyl alcohol)," *Phys. Rev. E* **59**, 5647–5654 (1999).
- ³⁸Y. Tamai and H. Tanaka, "Structure and Dynamics of Poly(Vinyl Alcohol) Hydrogel," *Mol. Simul.* **21**, 283–301 (1999).
- ³⁹G. E. Karlsson, T. S. Johansson, U. W. Gedde, and M. S. Hedenqvist, "Physical properties of dense amorphous poly(vinyl alcohol) as revealed by molecular dynamics simulation," *J. Macromol. Sci. Phys.* **41**, 185–206 (2002).
- ⁴⁰G. E. Karlsson, U. W. Gedde, and M. S. Hedenqvist, "Molecular dynamics simulation of oxygen diffusion in dry and water-containing poly(vinyl alcohol)," *Polymer* **45**, 3893–3900 (2004).
- ⁴¹E. Chiessi, F. Cavaliere, and G. Paradossi, "Supercooled Water in PVA Matrices. II. A Molecular Dynamics Simulation Study and Comparison with QENS Results," *J. Phys. Chem. B* **109**, 8091–8096 (2005).
- ⁴²E. Chiessi, F. Cavaliere, and G. Paradossi, "Water and Polymer Dynamics in Chemically Cross-Linked Hydrogels of Poly(vinyl alcohol): A Molecular Dynamics Simulation Study," *J. Phys. Chem. B* **111**, 2820–2827 (2007).
- ⁴³Q. G. Zhang, Q. L. Liu, Y. Chen, J. Y. Wu, and A. M. Zhu, "Microstructure dependent diffusion of water–ethanol in swollen poly(vinyl alcohol): A molecular dynamics simulation study," *Chem. Eng. Sci.* **64**, 334–340 (2009).
- ⁴⁴C. Wu, "Cooperative behavior of poly(vinyl alcohol) and water as revealed by molecular dynamics simulations," *Polymer* **51**, 4452–4460 (2010).
- ⁴⁵G. Tesei, G. Paradossi, and E. Chiessi, "Poly(vinyl alcohol) Oligomer in Dilute Aqueous Solution: A Comparative Molecular Dynamics Simulation Study," *J. Phys. Chem. B* **116**, 10008–10019 (2012).
- ⁴⁶W. Sun, H. Wu, Y. Luo, B. Li, L. Mao, X. Zhao, L. Zhang, and Y. Gao, "Structure and dynamics behavior during the glass transition of the polyisoprene in the presence of pressure: A molecular dynamics simulation," *Polymer* **238**, 124433 (2022).
- ⁴⁷R. Nagumo, K. Akamatsu, R. Miura, A. Suzuki, N. Hatakeyama, H. Takaba, and A. Miyamoto, "Computational Chemistry Study on the Microscopic Interactions between Biomolecules and Hydrophilic Polymeric Materials," *J. Chem. Engn. Japan* **46**, 421–423 (2013).
- ⁴⁸R. Nagumo, A. Shimizu, S. Iwata, and H. Mori, "Molecular dynamics study of the molecular mobilities and side-chain terminal affinities of 2-methoxyethyl acrylate and 2-hydroxyethyl methacrylate," *Polym. J.* **51**, 365–370 (2019).
- ⁴⁹R. Nagumo, T. Matsuoka, and S. Iwata, "Interactions between Acrylate/Methacrylate Biomaterials and Organic Foulants Evaluated by Molecular Dynamics Simulations of Simplified Binary Mixtures," *ACS Biomater. Sci. Eng.* **7**, 3709–3717 (2021).
- ⁵⁰N. Yasoshima, M. Fukuoka, H. Kitano, S. Kagaya, T. Ishiyama, and M. Gemmei-Ide, "Diffusion-Controlled Recrystallization of Water Sorbed into Poly(meth)acrylates Revealed by Variable-Temperature Mid-Infrared Spectroscopy and Molecular Dynamics Simulation," *J. Phys. Chem. B* **121**, 5133–5141 (2017).
- ⁵¹S. Kishinaka, A. Morita, and T. Ishiyama, "Molecular structure and vibrational spectra at water/poly(2-methoxyethylacrylate) and water/poly(methyl methacrylate) interfaces: A molecular dynamics simulation study," *J. Chem. Phys.* **150**, 044707 (2019).
- ⁵²A.-T. Kuo, S. Urata, R. Koguchi, K. Yamamoto, and M. Tanaka, "Analyses of equilibrium water content and blood compatibility for Poly(2-methoxyethyl acrylate) by molecular dynamics simulation," *Polymer* **170**, 76–84 (2019).
- ⁵³A.-T. Kuo, T. Sonoda, S. Urata, R. Koguchi, S. Kobayashi, and M. Tanaka, "Elucidating the Feature of Intermediate Water in Hydrated Poly(ω -methoxyalkyl acrylate)s by Molecular Dynamics Simulation and Differential Scanning Calorimetry Measurement," *ACS Biomater. Sci. Eng.* **6**, 3915–3924 (2020).
- ⁵⁴A.-T. Kuo, S. Urata, R. Koguchi, T. Sonoda, S. Kobayashi, and M. Tanaka, "Molecular Dynamics Study on the Water Mobility and Side-Chain Flexibility of Hydrated Poly(ω -methoxyalkyl acrylate)s," *ACS Biomater. Sci. Eng.* **6**, 6690–6700 (2020).
- ⁵⁵A.-T. Kuo, S. Urata, R. Koguchi, T. Sonoda, S. Kobayashi, and M. Tanaka, "Effects of Side-Chain Spacing and Length on Hydration States of Poly(2-methoxyethyl acrylate) Analogues: A Molecular Dynamics Study," *ACS Biomater. Sci. Eng.* **7**, 2383–2391 (2021).
- ⁵⁶N. Yasoshima, T. Ishiyama, M. Gemmei-Ide, and N. Matubayasi, "Molecular Structure and Vibrational Spectra of Water Molecules Sorbed in Poly(2-methoxyethylacrylate) Revealed by Molecular Dynamics Simulation," *J. Phys. Chem. B* **125**, 12095–12103 (2021).
- ⁵⁷N. Yasoshima, T. Ishiyama, and N. Matubayasi, "Adsorption Energetics of Amino Acid Analogs on Polymer/Water Interfaces Studied by All-Atom Molecular Dynamics Simulation and a Theory of Solutions," *J. Phys. Chem. B* **126**, 4389–4400 (2022).
- ⁵⁸Y. Ikemoto, Y. Harada, M. Tanaka, S.-n. Nishimura, D. Murakami, N. Kurahashi, T. Moriwaki, K. Yamazoe, H. Washizu, Y. Ishii, and H. Torii, "Infrared Spectra and Hydrogen-Bond Configurations of Water Molecules at the Interface of Water-Insoluble Polymers under Humidified Conditions," *J. Phys. Chem. B* **126**, 4143–4151 (2022).
- ⁵⁹H. O. S. Yadav, A.-T. Kuo, S. Urata, K. Funahashi, Y. Imamura, and W. Shinoda, "Adsorption characteristics of peptides on ω -functionalized self-assembled monolayers: A molecular dynamics study," *Phys. Chem. Chem. Phys.* **24**, 14805–14815 (2022).
- ⁶⁰R. Nagumo, Y. Suzuki, I. Nakata, T. Matsuoka, and S. Iwata, "Influence of Molecular Structures of Organic Foulants on the Antifouling Properties of Poly(2-methoxyethyl acrylate) and Its Analogs: A Molecular Dynamics Study," *ACS Biomater. Sci. Eng.* **9**, 4269–4276 (2023).
- ⁶¹K. Shikata, T. Kikutsuji, N. Yasoshima, K. Kim, and N. Matubayasi, "Revealing the hidden dynamics of confined water in acrylate polymers: Insights from hydrogen-bond lifetime analysis," *J. Chem. Phys.* **158**, 174901 (2023).
- ⁶²H. O. S. Yadav, R. Chauhan, and A.-T. Kuo, "Hydration characteristics of blood-compatible poly(2-methoxyethyl acrylate) (PMEA) polymer chains at infinite dilution," *Mol. Simul.* **51**, 179–187 (2025).
- ⁶³H. O. S. Yadav, A.-T. Kuo, S. Urata, K. Funahashi, Y. Imamura, and W. Shinoda, "Hydrophobicity-Governed Protein Adsorption on Poly(ω -methoxyalkyl acrylate) Surfaces: A Coarse-Grained Molecular Dynamics Study," *J. Chem. Theory Comput.* **21**, 10561–10573 (2025).
- ⁶⁴M. Gemmei-Ide, R. Tomita, K. Kuroda, N. Yasoshima, S. Kagaya, and T. Ishiyama, "Weak Water–Polymer Interactions Govern Water Recrystallization in Nonwater-Soluble Polymers with High Glass Transition Temperature," *J. Phys. Chem. B* **129**, 11574–11583 (2025).
- ⁶⁵C. A. Kreck and R. L. Mancera, "Characterization of the Glass Transition of Water Predicted by Molecular Dynamics Simulations Using Nonpolarizable Intermolecular Potentials," *J. Phys. Chem. B* **118**, 1867–1880 (2014).
- ⁶⁶"J-OCTA - an integrated system for multiscale modeling and simulation | JSOL Corporation," <https://www.j-octa.com/>.
- ⁶⁷W. L. Jorgensen, D. S. Maxwell, and J. Tirado-Rives, "Development and Testing of the OPLS All-Atom Force Field on Conformational Energetics and Properties of Organic Liquids," *J. Am. Chem. Soc.* **118**, 11225–11236 (1996).
- ⁶⁸H. Kojima, K. Handa, K. Yamada, and N. Matubayasi, "Water Dissolved in a Variety of Polymers Studied by Molecular Dynamics Simulation and a Theory of Solutions," *J. Phys. Chem. B* **125**, 9357–9371 (2021).
- ⁶⁹J. L. F. Abascal and C. Vega, "A general purpose model for the condensed phases of water: TIP4P/2005," *J. Chem. Phys.* **123**, 234505 (2005).
- ⁷⁰M. J. Abraham, T. Murtola, R. Schulz, S. Páll, J. C. Smith, B. Hess, and E. Lindahl, "GROMACS: High performance molecular simulations through multi-level parallelism from laptops to supercomputers," *SoftwareX* **1–2**, 19–25 (2015).
- ⁷¹L. Martínez, R. Andrade, E. G. Birgin, and J. M. Martínez, "PACKMOL: A package for building initial configurations for molecular dynamics simulations," *J. Comput. Chem.* **30**, 2157–2164 (2009).
- ⁷²G. Bussi, D. Donadio, and M. Parrinello, "Canonical sampling through velocity rescaling," *J. Chem. Phys.* **126**, 014101 (2007).
- ⁷³M. Bernetti and G. Bussi, "Pressure control using stochastic cell rescaling," *J. Chem. Phys.* **153**, 114107 (2020).
- ⁷⁴R. S. Singh, J. W. Biddle, P. G. Debenedetti, and M. A. Anisimov, "Two-state thermodynamics and the possibility of a liquid-liquid phase transition in supercooled TIP4P/2005 water," *J. Chem. Phys.* **144**, 144504 (2016).
- ⁷⁵J. W. Biddle, R. S. Singh, E. M. Sparano, F. Ricci, M. A. González, C. Valeriani, J. L. F. Abascal, P. G. Debenedetti, M. A. Anisimov, and F. Caupin,

- “Two-structure thermodynamics for the TIP4P/2005 model of water covering supercooled and deeply stretched regions,” *J. Chem. Phys.* **146**, 034502 (2017).
- ⁷⁶S. Saito, B. Bagchi, and I. Ohmine, “Crucial role of fragmented and isolated defects in persistent relaxation of deeply supercooled water,” *J. Chem. Phys.* **149**, 124504 (2018).
- ⁷⁷Abraham. Savitzky and M. J. E. Golay, “Smoothing and Differentiation of Data by Simplified Least Squares Procedures,” *Anal. Chem.* **36**, 1627–1639 (1964).
- ⁷⁸T. G. Fox, “Influence of Diluent and of Copolymer Composition on the Glass Temperature of a Polymer System,” *Bull. Am. Phys. Soc.* **1**, 123 (1956).
- ⁷⁹A. Soldera and N. Metatla, “Glass transition of polymers: Atomistic simulation versus experiments,” *Phys. Rev. E* **74**, 061803 (2006).
- ⁸⁰B. C. Hancock and G. Zografi, “The Relationship Between the Glass Transition Temperature and the Water Content of Amorphous Pharmaceutical Solids,” *Pharm. Res.* **11**, 471–477 (1994).
- ⁸¹J. Rault, R. Gref, Z. H. Ping, Q. T. Nguyen, and J. Néel, “Glass transition temperature regulation effect in a poly(vinyl alcohol)—water system,” *Polymer* **36**, 1655–1661 (1995).
- ⁸²A. Kyritsis and P. Pissis, “Dielectric studies of polymer-water interactions and water organization in PEO/water systems,” *J. Polym. Sci. B Polym. Phys.* **35**, 1545–1560 (1997).
- ⁸³A. Kyritsis, P. Pissis, J. L. Gómez Ribelles, and M. Monleón Pradas, “Dielectric relaxation spectroscopy in PHEA hydrogels,” *J. Non-Cryst. Solids* **172–174**, 1041–1046 (1994).
- ⁸⁴J. Verhoeven, R. Schaeffer, J. A. Bouwstra, and H. E. Junginger, “The physico-chemical characterization of poly (2-hydroxyethyl methacrylate-co-methacrylic acid: 2. Effect of water, PEG 400 and PEG 6000 on the glass transition temperature,” *Polymer* **30**, 1946–1950 (1989).
- ⁸⁵J. A. Bouwstra, M. A. Salomons-de Vries, and J. C. van Miltenburg, “The thermal behaviour of water in hydrogels,” *Thermochim. Acta* **248**, 319–327 (1995).
- ⁸⁶J. R. Meakin, D. W. L. Hukins, C. T. Imrie, and R. M. Aspden, “Thermal analysis of poly(2-hydroxyethyl methacrylate) (pHEMA) hydrogels,” *J. Mater. Sci. Mater. Med.* **14**, 9–15 (2003).
- ⁸⁷A. Luzar and D. Chandler, “Effect of Environment on Hydrogen Bond Dynamics in Liquid Water,” *Phys. Rev. Lett.* **76**, 928–931 (1996).
- ⁸⁸A. Luzar and D. Chandler, “Hydrogen-bond kinetics in liquid water,” *Nature* **379**, 55–57 (1996).
- ⁸⁹A. Luzar, “Resolving the hydrogen bond dynamics conundrum,” *J. Chem. Phys.* **113**, 10663–10675 (2000).
- ⁹⁰N. B. Graham, M. Zulfiqar, N. E. Nwachuku, and A. Rashid, “Interaction of poly(ethylene oxide) with solvents: 2. Water-poly(ethylene glycol),” *Polymer* **30**, 528–533 (1989).
- ⁹¹M. J. Hey and S. M. Ilett, “Poly(ethylene oxide) hydration studied by differential scanning calorimetry,” *J. Chem. Soc., Faraday Trans.* **87**, 3671–3675 (1991).
- ⁹²L. Huang and K. Nishinari, “Interaction between poly(ethylene glycol) and water as studied by differential scanning calorimetry,” *J. Polym. Sci. B Polym. Phys.* **39**, 496–506 (2001).
- ⁹³M. Nakanishi and R. Nozaki, “Systematic study of the glass transition in polyhydric alcohols,” *Phys. Rev. E* **83**, 051503 (2011).
- ⁹⁴R. G. M. Van Der Sman, “Predictions of Glass Transition Temperature for Hydrogen Bonding Biomaterials,” *J. Phys. Chem. B* **117**, 16303–16313 (2013).
- ⁹⁵T. Jin, C. W. Coley, and A. Alexander-Katz, “Molecular signatures of the glass transition in polymers,” *Phys. Rev. E* **106**, 014506 (2022).
- ⁹⁶T. Jin, C. W. Coley, and A. Alexander-Katz, “A Computationally Informed Unified View on the Effect of Polarity and Sterics on the Glass Transition in Vinyl-based Polymer Melts,” *ACS Macro Lett.* **12**, 1517–1522 (2023).
- ⁹⁷D. Rapaport, “Hydrogen bonds in water: Network organization and lifetimes,” *Mol. Phys.* **50**, 1151–1162 (1983).
- ⁹⁸J.-P. Hansen and I. R. McDonald, *Theory of Simple Liquids: With Applications of Soft Matter*, 4th ed. (Elsevier, Amstersdam, 2013).

Supplementary Material

Classification of interfacial water governed by water-polymer interactions in hydrated polymers: A molecular dynamics simulation study of ethylene-based and acrylate polymers

Atsuki Hashimoto, Kokoro Shikata, Kang Kim, and Nobuyuki Matubayasi

*Division of Chemical Engineering, Graduate School of Engineering Science, The University of Osaka, Toyonaka, Osaka
560-8531, Japan*

TABLE S1. The water solubility, equilibrium water content, glass transition temperature in the dry state T_g , blood compatibility, and presence or absence of intermediate water for polymers examined in this study.

	PEG	PMEA	PMEMA	PVA	PHEA	PHEMA	PBA
water solubility	+	-	-	+	-	-	-
equilibrium water content [wt%]		9.0 ^{S1}	4.2 ^{S1}		60 ^{S1}	39 ^{S1}	1.9 ^{S1}
glass transition temperature in the dry state T_g [°C]	-51 ^{S2}	-35 ^{S3}	26 ^{S3}	85 ^{S4}	15.2 ^{S5}	115 ^{S6}	-47 ^{S3}
platelet adhesion inhibition	+ ^{S7}	+ ^{S1}	-	-	-	-	-
intermediate water	+ ^{S8}	+ ^{S1}	-	-	-	-	-

TABLE S2. System equilibration protocol. At step 4, the heating process of 300 → 500 K and the subsequent cooling process 500 → 300 K each required 100 ps. This temperature cycling was repeated 10 times.

Step	Run	Time (ns)	Temperature (K)	Pressure (bar)
1	<i>NVT</i>	1	1000	-
2	<i>NPT</i>	1	1000	1000
3	<i>NPT</i>	1.5	1000 → 300	1000
4	<i>NPT</i>	2	300 ⇌ 500	1
5	<i>NPT</i>	10	300	1000
6	<i>NPT</i>	10	300	1
7	<i>NPT</i>	5	600 or 500	1

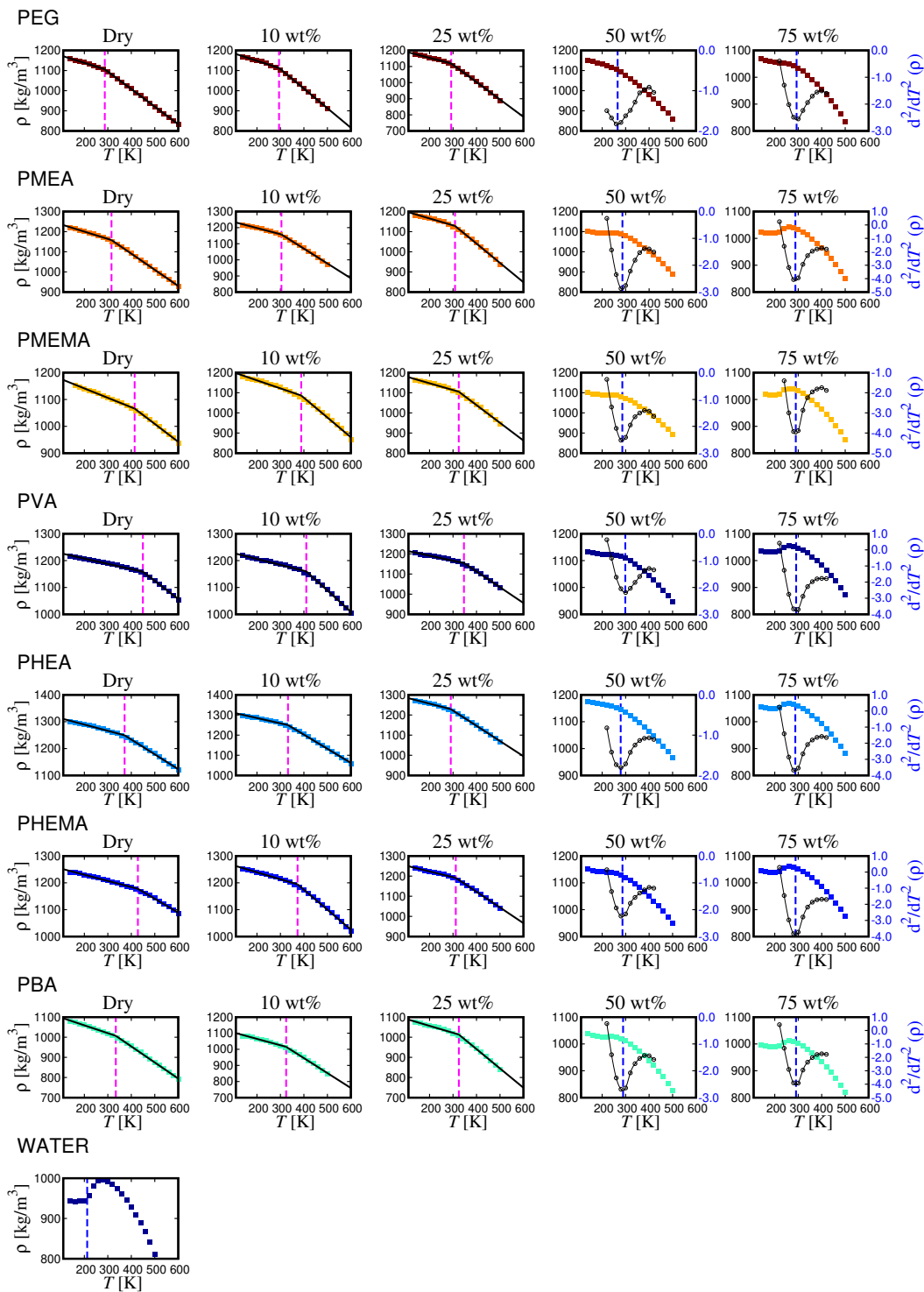


FIG. S1. Temperature dependence of mass density ρ (left vertical axis). The magenta dashed line indicates the glass transition temperature T_g . For water contents below 25 wt%, T_g is determined from the intersection of two straight line fits (black lines). In contrast, for water contents above 50 wt%, T_g is defined as the temperature at which the second derivative using the right vertical axis, obtained from spline interpolation, reaches a minimum. In the pure water system, the blue dashed line denotes the previously reported glass transition temperature of 212 K obtained from MD simulations.^{S9}

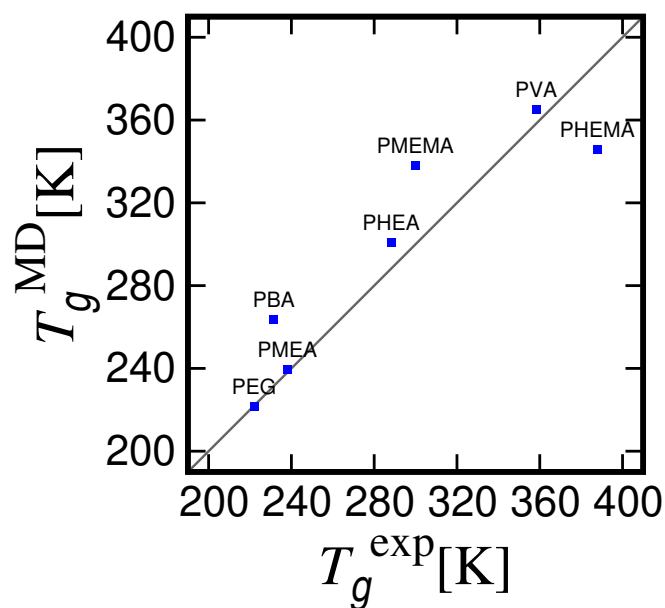


FIG. S2. Relationship between the corrected glass transition temperature T_g^{MD} and the experimental values T_g^{exp} .

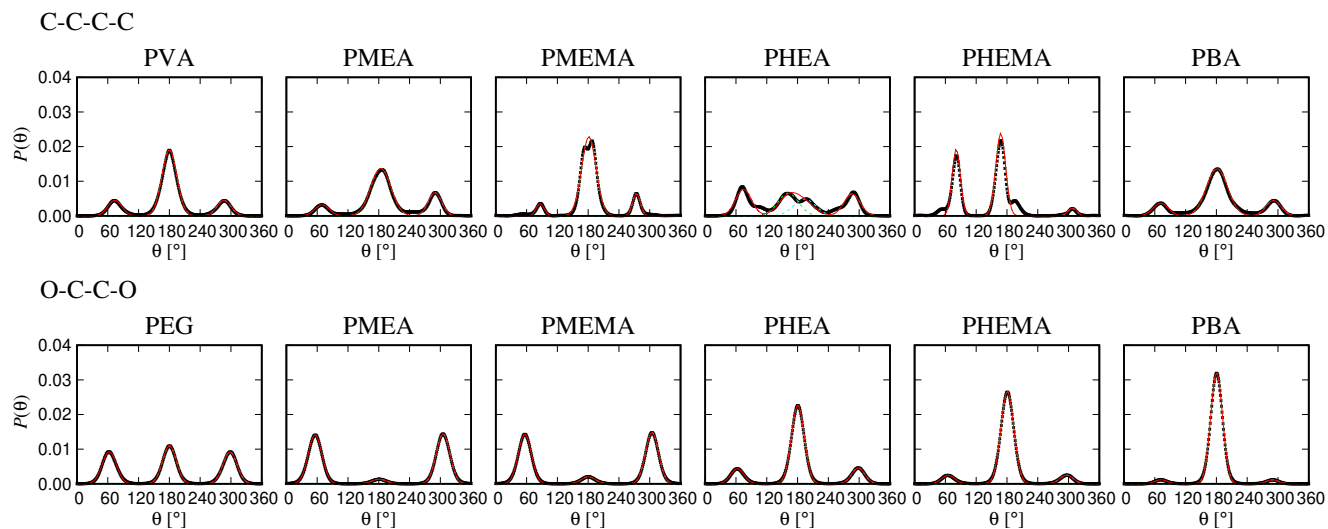


FIG. S3. Distribution functions of polymer dihedral angles: (top) dihedral angles of the main chain carbon backbone (C-C-C-C) and (bottom) dihedral angles of carbon skeleton substituted with oxygen atoms (O-C-C-O). For PBA, the corresponding dihedral angle of the butyl side chain. Temperature: 300 K; water content: 25 wt%. The black lines represent simulation data, and the red lines denote Gaussian mixture model fits.

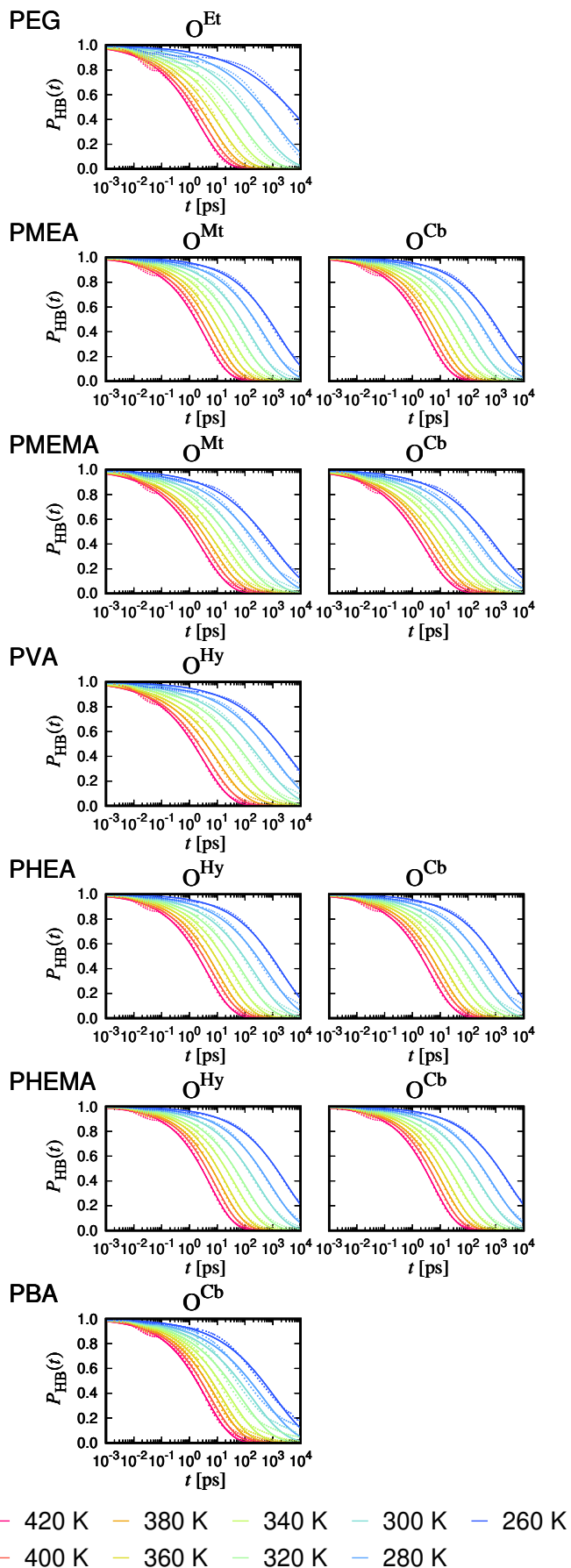


FIG. S4. H-bond time correlation function $P_{\text{HB}}(t)$ obtained from 260 to 420 K at 20 K intervals. The acceptor oxygen atoms involved in H-bonding with water molecules are denoted as ether oxygen (O^{Et}), methoxy oxygen (O^{Mt}), hydroxyl oxygen (O^{Hy}), and carbonyl oxygen (O^{Cb}). Solid lines represent fits to the KWW function, $P_{\text{HB}}(t) \approx \exp[-(t/\tau_{\text{KWW}})^{\beta_{\text{KWW}}}]$.

- [S1]M. Tanaka and A. Mochizuki, *J. Biomed. Mater. Res. A* **68A**, 684 (2004).
- [S2]C. Trotzig, S. Abrahmsén-Alami, and F. H. J. Maurer, *Polymer* **48**, 3294 (2007).
- [S3]K. Sato, S. Kobayashi, M. Kusakari, S. Watahiki, M. Oikawa, T. Hoshiba, and M. Tanaka, *Macromol. Biosci.* **15**, 1296 (2015).
- [S4]R. M. Hodge, T. J. Bastow, G. H. Edward, G. P. Simon, and A. J. Hill, *Macromolecules* **29**, 8137 (1996).
- [S5]M. Salmerón Sánchez, G. G. Ferrer, M. Monleón Pradas, and J. L. Gómez Ribelles, *Macromolecules* **36**, 860 (2003).
- [S6]W. E. Roorda, J. A. Bouwstra, M. A. de Vries, and H. E. Junginger, *Biomaterials* **9**, 494 (1988).
- [S7]M. J. Santos-Martinez, K. Rahme, J. J. Corbalan, C. Faulkner, J. D. Holmes, L. Tajber, C. Medina, and M. W. Radomski, *J. Biomed. Nanotechnol.* **10**, 1004 (2014).
- [S8]T. Hatakeyma, H. Kasuga, M. Tanaka, and H. Hatakeyama, *Thermochim. Acta* **465**, 59 (2007).
- [S9]C. A. Kreck and R. L. Mancera, *J. Phys. Chem. B* **118**, 1867 (2014).